Available online at www.eccomasproceedia.org
Eccomas Proceedia COMPDYN (2025) 5525-55 6

ECCOMAS
Proceedia

COMPDYN 2025
10th ECCOMAS Thematic Conference on
Computational Methods in Structural Dynamics and Earthquake Engineering
M. Papadrakakis, M. Fragiadakis (eds.)
Rhodes Island, Greece, 15-18 June 2025

DATA-DRIVEN MODELING OF STRUCTURAL DYNAMICS: IMPROVING MEASUREMENT NOISE ROBUSTNESS WITH AUGMENTED DYNAMIC MODE DECOMPOSITION

M. A. Abdennadher[1], F. Williams-Riquer[1], D. A. Dao[1], J. Grabe[1]

[1]Hamburg University of Technology
Institute of Geotechnical Engineering and Construction Management, Schellerdamm 22-24, 21079 Hamburg
e-mail: mohamed.abdennadher@tuhh.de

Abstract. *Accurate modeling of structural dynamics is essential for designing effective vibration control strategies in earthquake engineering. Traditional system identification techniques often struggle to distinguish intrinsic structural behavior from external forces, particularly in the presence of measurement noise. Dynamic Mode Decomposition with Control (DMDc) offers a data-driven approach to extracting system dynamics while accounting for external inputs. However, its performance degrades significantly in noisy environments, leading to inaccurate mode identification and misrepresented damping characteristics. To address this challenge, we introduce Augmented Dynamic Mode Decomposition with Control (AugDMDc), a novel extension that incorporates time-delay coordinates into DMDc to enhance noise robustness. By embedding past measurements into the state-space representation, AugDMDc effectively reduces the impact of sensor noise while preserving the ability to separate a structure's natural response from external excitations. We validate this approach using a structural dynamic system equipped with an Active Mass Damper (AMD), comparing the performance of DMDc and AugDMDc under various conditions.*

Keywords: Dynamic Mode Decomposition (DMD), DMD with Control (DMDc), Augmented DMDc (AugDMDc), Measurement Noise Robustness, Time-Delay Coordinates, System Identification

ISSN:2623-3347
Peer-review under responsibility of the organizing committee of COMPDYN 2025.
doi: 10.7712/120125.128 0.24480

1 Introduction

Predicting, controlling, and mitigating vibrations in structures subjected to seismic forces is a key challenge in structural engineering. Earthquakes introduce dynamic forces that induce oscillations capable of compromising structural integrity, leading to extensive damage or, in extreme cases, catastrophic collapse. Over the decades, engineers have introduced an array of strategies to counteract these effects, ranging from passive systems such as tuned mass dampers to active control mechanisms employing real-time actuators [1, 2, 3, 4, 5, 6, 7, 8]. These approaches aim to stabilize structures, dissipate energy, and safeguard both human lives and infrastructure. Yet, the efficacy of such methods rests heavily on the precision of the dynamic models employed to forecast a structure's response to seismic loads. Accurately capturing the interplay between a building's intrinsic behavior and the external forces it encounters remains a challenge that demands robust, data-driven methodologies.

A central difficulty in constructing reliable dynamic models lies in isolating the intrinsic dynamics of a system from the influence of external inputs, such as seismic forces or wind gusts. Measurement data—typically acquired via accelerometers, strain gauges, or other sensors—often reflect a combination of these factors, complicating efforts to isolate the evolution of the system's natural behavior [9, 10]. Traditional modeling techniques, including finite element methods and classical system identification approaches like subspace methods, frequently rely on simplifying assumptions that fail to fully account for this complexity [11]. Consequently, these methods may produce representations that inadequately distinguish between forced responses and the structure's inherent oscillatory modes, undermining their utility for control design.

In recent years, data-driven techniques have emerged as powerful tools to address these limitations, with Dynamic Mode Decomposition (DMD) gaining prominence for its ability to extract coherent spatiotemporal patterns from high-dimensional datasets [12, 13]. Originally developed in the fluid dynamics community, DMD approximates a system's evolution as a linear superposition of modes, offering a computationally efficient means to characterize dynamics without requiring an explicit governing equation. However, standard DMD assumes autonomous system behavior, making it unsuited for scenarios involving external actuation—a critical limitation in structural engineering applications where seismic inputs or control forces are prevalent.

To overcome this shortfall, Dynamic Mode Decomposition with Control (DMDc) extends the DMD framework by explicitly incorporating the effects of external inputs [14]. DMDc constructs a low-order model that simultaneously identifies the state-space dynamics and the input matrix, enabling a clearer separation between a system's intrinsic behavior and its response to external forcing. This capability renders DMDc particularly promising for structural control applications, where distinguishing seismic effects from a building's natural dynamics is paramount for designing effective mitigation strategies. Studies such as those by [15] and [16] have demonstrated DMDc's versatility across diverse domains, from fluid-structure interactions to robotics, underscoring its potential for engineering systems subject to controlled or uncontrolled inputs.

Despite its advantages, DMDc inherits a well-documented weakness of the original DMD algorithm: sensitivity to measurement noise [17, 18]. In real-world structural monitoring, data collected from accelerometers or other sensors are invariably corrupted by noise arising from environmental interference, sensor limitations, or signal processing artifacts. This noise can significantly distort the identified modes and eigenvalues, leading to models that misrepresent

the true system dynamics. For instance, noisy data may exaggerate damping ratios or shift resonant frequencies, compromising the reliability of downstream control strategies. This vulnerability has spurred ongoing research into noise-robust variants of DMD and DMDc, with approaches such as total least-squares DMD [19] and Forward-Backward Extended DMD [20] gaining traction in the literature.

Building on this foundation, we propose an enhanced approach that combines DMDc with time-delay coordinates to improve system identification in the presence of noise. Specifically, we apply this methodology to the challenge of modeling structural dynamics under controlled excitations, where accurate separation of intrinsic and external effects is critical. This work seeks to advance the applicability of DMDc-based techniques in structural engineering, offering a more reliable tool for designing control strategies that mitigate vibrational responses. To further enhance DMD's capabilities, we incorporate Augmented Dynamic Mode Decomposition (AugDMD), first proposed by [13], which uses time-delay coordinates to improve DMD's ability to capture nonlinear dynamics. We extend this approach by integrating AugDMD with DMDc (AugDMDc), offering a more robust framework for handling noisy data in structural dynamics and improving the separation of intrinsic dynamics and external excitations in seismic environments.

2 Dynamic Mode Decomposition

This section summarizes the standard DMD [12, 21, 22] algorithm and its extensions AugDMD [13] using time-delay coordinates, DMDc [14] considering the measured input signal, and the novel AugDMDc formulation combining DMDc and AugDMD. The DMD algorithm provides a spatiotemporal data analysis, identifying dynamic modes (DMD modes) from collected snapshots or measurements of a dynamical system.

The standard DMD method considers a set of snapshot data vectors $\mathbf{x}(k) \in \mathbb{R}^n$ obtained at discrete time steps k from a dynamical system described by

$$\mathbf{x}(k+1) = \mathbf{A}\mathbf{x}(k), \tag{1}$$

where $\mathbf{A}$ is an unknown operator and $k \in \{0, 1, \ldots, m\}$. The purpose of DMD is to approximate the eigenvectors and eigenvalues of $\mathbf{A}$. The procedure can be summarized in the following steps:

1. **Snapshot matrix formation:** Construct two snapshot data matrices from m snapshots:

$$\mathbf{X}_1 = [\mathbf{x}(1) \quad \mathbf{x}(2) \quad \ldots \quad \mathbf{x}(m-1)], \tag{2a}$$
$$\mathbf{X}_2 = [\mathbf{x}(2) \quad \mathbf{x}(3) \quad \ldots \quad \mathbf{x}(m)], \tag{2b}$$

   where $\mathbf{X}_1, \mathbf{X}_2 \in \mathbb{R}^{n\times(m-1)}$.

2. **Truncated Singular Value Decomposition (SVD):** Compute the rank-r truncated economy SVD of $\mathbf{X}_1$:

$$\mathbf{X}_1 \approx \widetilde{\mathbf{U}}\widetilde{\mathbf{\Sigma}}\widetilde{\mathbf{V}}^*, \tag{3}$$

   where $\widetilde{\mathbf{U}} \in \mathbb{C}^{n\times r}$, $\widetilde{\mathbf{\Sigma}} \in \mathbb{C}^{r\times r}$, $\widetilde{\mathbf{V}} \in \mathbb{C}^{m\times r}$, r is the rank of $\mathbf{X}_1$, and * denotes conjugate transpose.

3. **Low-dimensional projection:** Project $\mathbf{A}$ onto an r-dimensional subspace spanned by $\widetilde{\mathbf{U}}$:

$$\widetilde{\mathbf{A}} = \widetilde{\mathbf{U}}^*\mathbf{A}\widetilde{\mathbf{U}} = \widetilde{\mathbf{U}}^*\mathbf{X}_2\widetilde{\mathbf{V}}\widetilde{\mathbf{\Sigma}}^{-1}. \tag{4}$$

4. **Reduced-order dynamical system:** Formulate a low-dimensional linear model:

$$\widetilde{\mathbf{x}}(k+1) = \widetilde{\mathbf{A}}\widetilde{\mathbf{x}}(k), \tag{5}$$

with the original state approximated as $\mathbf{x}(k) = \widetilde{\mathbf{U}}\widetilde{\mathbf{x}}(k)$.

5. **Eigenvalue decomposition:** Compute the eigendecomposition of $\widetilde{\mathbf{A}}$:

$$\widetilde{\mathbf{A}}\mathbf{W} = \mathbf{W}\mathbf{\Lambda}, \tag{6}$$

where the columns of $\mathbf{W}$ are eigenvectors and $\mathbf{\Lambda}$ is a diagonal matrix with eigenvalues λ_k.

6. **Reconstruction of original eigenvectors (DMD modes):** The eigenvalues of $\mathbf{A}$ are approximated directly by those of $\widetilde{\mathbf{A}}$, and the corresponding DMD modes are given by

$$\mathbf{\Phi} = \mathbf{X}_2\widetilde{\mathbf{V}}\widetilde{\mathbf{\Sigma}}^{-1}\mathbf{W}. \tag{7}$$

Finally, the continuous-time approximation of the system state can be expressed as

$$\mathbf{x}(t) \approx \sum_{k=1}^{r} \varphi_k \exp(\omega_k t) b_k = \mathbf{\Phi}\exp(\mathbf{\Omega}t)\mathbf{b}, \tag{8}$$

where b_k are coefficients determined by the initial condition projected onto each mode, the columns of $\mathbf{\Phi}$ are the DMD modes φ_k, and $\mathbf{\Omega}$ is a diagonal matrix containing continuous-time eigenvalues $\omega_k = \ln(\lambda_k)/\Delta t$.

2.1 Augmented DMD (AugDMD)

To improve the robustness of DMD when dealing with complex and noisy systems, the Augmented Dynamic Mode Decomposition (AugDMD) considers time-delay coordinates based on Takens' embedding theorem [23]. This theorem suggests that the intrinsic dynamics of specific systems can be effectively reconstructed from a finite number of observations using time-delayed embeddings [13]. AugDMD closely follows the standard DMD methodology but instead utilizes augmented snapshot matrices defined as

$$\mathbf{X}_{1\,\text{aug}} = \begin{bmatrix} \mathbf{x}(1) & \mathbf{x}(2) & \cdots & \mathbf{x}(m-s) \\ \mathbf{x}(2) & \mathbf{x}(3) & \cdots & \mathbf{x}(m-s+1) \\ \vdots & \vdots & \ddots & \vdots \\ \mathbf{x}(s) & \mathbf{x}(s+1) & \cdots & \mathbf{x}(m-1) \end{bmatrix}, \tag{9a}$$

$$\mathbf{X}_{2\,\text{aug}} = \begin{bmatrix} \mathbf{x}(2) & \mathbf{x}(3) & \cdots & \mathbf{x}(m-s+1) \\ \mathbf{x}(3) & \mathbf{x}(4) & \cdots & \mathbf{x}(m-s+2) \\ \vdots & \vdots & \ddots & \vdots \\ \mathbf{x}(s+1) & \mathbf{x}(s+2) & \cdots & \mathbf{x}(m) \end{bmatrix}, \tag{9b}$$

where s is the number of delay coordinates and $\mathbf{X}_{1\,\text{aug}}, \mathbf{X}_{2\,\text{aug}} \in \mathbb{R}^{(s\cdot n)\times(m-s)}$.

2.2 DMD with control (DMDc)

DMDc extends the traditional DMD framework by explicitly incorporating control inputs. This approach distinguishes the intrinsic system dynamics from the external influences due to actuated inputs, resulting in a disambiguated input-output model representation [14]. The following summary of this methodology is based on [14].

The objective of DMDc is to describe the relationship between $\mathbf{x}(k+1)$, $\mathbf{x}(k)$ and the current control $\mathbf{u}(k)$. This relationship is provided by the linear operators $\mathbf{A}$ and $\mathbf{B}$ as follows

$$\mathbf{x}(k+1) \approx \mathbf{A}\mathbf{x}(k) + \mathbf{B}\mathbf{u}(k), \tag{10}$$

where $\mathbf{x}(k) \in \mathbb{R}^n$, $\mathbf{u}(k) \in \mathbb{R}^l$, $\mathbf{A} \in \mathbb{R}^{n\times n}$, and $\mathbf{B} \in \mathbb{R}^{n\times l}$. Similar to standard DMD, data matrices are constructed as in Eq. 2a and Eq. 2b. Consider additionally a new sequence of collected control input snapshots as

$$\boldsymbol{\Upsilon} = \begin{bmatrix} \mathbf{u}(1) & \mathbf{u}(2) & \dots & \mathbf{u}(m-1) \end{bmatrix}, \tag{11}$$

where $\boldsymbol{\Upsilon} \in \mathbb{R}^{(m-1)\times l}$. Rewrite Eq. 10 in matrix form including the data matrices in Eq. 2a and Eq. 2b and Eq. 11 as

$$\mathbf{X}_2 \approx \mathbf{A}\mathbf{X}_1 + \mathbf{B}\boldsymbol{\Upsilon}. \tag{12}$$

Focus on the general case where both linear operators $\mathbf{A}$ and $\mathbf{B}$ are unknown. Rewrite the system in Eq. 12 as

$$\mathbf{X}_2 \approx \mathbf{G}\boldsymbol{\Omega}, \tag{13}$$

where $\mathbf{G} = \begin{bmatrix} \mathbf{A} & \mathbf{B} \end{bmatrix}$ and $\boldsymbol{\Omega} = \begin{bmatrix} \mathbf{X}_1 & \boldsymbol{\Upsilon} \end{bmatrix}^T$. The operator $\mathbf{G}$ is obtained using the pseudo inverse as

$$\mathbf{G} = \mathbf{X}_2\boldsymbol{\Omega}^\dagger. \tag{14}$$

To solve the least-squares problem in Eq. 14, a truncated SVD of the augmented matrix $\boldsymbol{\Omega}$ is performed

$$\boldsymbol{\Omega} \approx \widetilde{\mathbf{U}}\widetilde{\boldsymbol{\Sigma}}\widetilde{\mathbf{V}}^*. \tag{15}$$

The truncation rank p for $\boldsymbol{\Omega}$ should generally exceed the truncation rank r used for $\mathbf{X}$. Thus, approximate $\mathbf{G}$ as

$$\mathbf{G} \approx \overline{\mathbf{G}} = \mathbf{X}_2\widetilde{\mathbf{V}}\widetilde{\boldsymbol{\Sigma}}^{-1}\widetilde{\mathbf{U}}^*. \tag{16}$$

To obtain the operators $\mathbf{A}$ and $\mathbf{B}$, we partition the columns of $\widetilde{\mathbf{U}}^*$ as $\widetilde{\mathbf{U}}^* = \begin{bmatrix} \widetilde{\mathbf{U}}_1^* & \widetilde{\mathbf{U}}_2^* \end{bmatrix}$ where $\widetilde{\mathbf{U}}_1 \in \mathbb{R}^{n\times p}$ corresponds to the states and $\widetilde{\mathbf{U}}_2 \in \mathbb{R}^{l\times p}$ corresponds to the input. Therefore one can separately estimate $\mathbf{A}$ and $\mathbf{B}$ as

$$[\mathbf{A},\, \mathbf{B}] \approx [\mathbf{X}_2\widetilde{\mathbf{V}}\widetilde{\boldsymbol{\Sigma}}^{-1}\widetilde{\mathbf{U}}_1^*, \quad \mathbf{X}_2\widetilde{\mathbf{V}}\widetilde{\boldsymbol{\Sigma}}^{-1}\widetilde{\mathbf{U}}_2^*]. \tag{17}$$

For the case of large-dimensional systems, directly using the computed $\mathbf{A}$ and $\mathbf{B}$ becomes computationally impractical. Instead, a second truncated SVD is perfromed, this time of the output matrix $\mathbf{X}_2 \approx \widehat{\mathbf{U}}\widehat{\boldsymbol{\Sigma}}\widehat{\mathbf{V}}^*$, selecting a lower rank r truncation ($r < p$). Define a reduced-order subspace via the linear transformation $\mathbf{x} = \widehat{\mathbf{U}}\widetilde{\mathbf{x}}$, and formulate a low-dimensional linear model using the operators

$$\widetilde{\mathbf{A}} = \widehat{\mathbf{U}}^*\mathbf{X}'\widetilde{\mathbf{V}}\widetilde{\boldsymbol{\Sigma}}^{-1}\widetilde{\mathbf{U}}_1^*\widehat{\mathbf{U}}, \tag{18}$$

$$\widetilde{\mathbf{B}} = \widehat{\mathbf{U}}^*\mathbf{X}'\widetilde{\mathbf{V}}\widetilde{\boldsymbol{\Sigma}}^{-1}\widetilde{\mathbf{U}}_2^*. \tag{19}$$

The resulting reduced-order system then takes the form of

$$\widetilde{\mathbf{x}}(k+1) = \widetilde{\mathbf{A}}\widetilde{\mathbf{x}}(k) + \widetilde{\mathbf{B}}\mathbf{u}(k). \tag{20}$$

The dynamic modes of the original system can be computed by performing the eigendecomposition $\widetilde{\mathbf{A}}\mathbf{W} = \mathbf{W}\mathbf{\Lambda}$. Finally the dynamic modes of $\mathbf{A}$ are given by

$$\mathbf{\Phi} = \mathbf{X}_2\widetilde{\mathbf{V}}\widetilde{\mathbf{\Sigma}}^{-1}\widetilde{\mathbf{U}}_1^*\widehat{\mathbf{U}}\mathbf{W}. \tag{21}$$

2.3 AugDMDc

We propose to combine AugDMD and DMDc to increase noise robustness for actuated systems by using the DMDc algorithm described in Sec. 2.2 and augment the data matrices in the same form described in Eq. 9. Since the scope focuses on applying DMD for structural dynamics problems where $n << m$, no rank truncation from either the new augmented $\mathbf{\Omega}_{\text{aug}}$ or $X_{2\,\text{aug}}$ is required. To apply the proposed AugDMDc, we first consider a number s of time-delay coordinates. We then deploy the normal DMDc without rank truncation when performing the SVD. For this case, we would only need one SVD to calculate the pseudoinverse as in Eq. 14. Consequently, we obtain an augmented system with $\mathbf{A}_{\text{aug}} \in \mathbb{R}^{(n\times s)\times(n\times s)}$ and $\mathbf{B}_{\text{aug}} \in \mathbb{R}^{(n\times s)\times l}$. $\mathbf{A}_{\text{aug}}$ consists of the first $n \times s$ columns of $\mathbf{G}_{\text{aug}}$ and $\mathbf{B}_{\text{aug}}$ of the rest (starting from $n \times s + 1$ until the end) of columns of $\mathbf{G}_{\text{aug}}$.

In the presence of noise, we have a tuning parameter s (number of time-delay coordinates) that we can adjust to improve our system's modeling and time-ahead prediction. Furthermore, AugDMDc keeps leveraging the DMDc's disambiguation capability to obtain a free response to the unactuated system and provides an augmented system capable of predicting the forced system's reaction to unprecedented input signals. Fig. 1 provides a schematic overview of the AugDMDc algorithm.

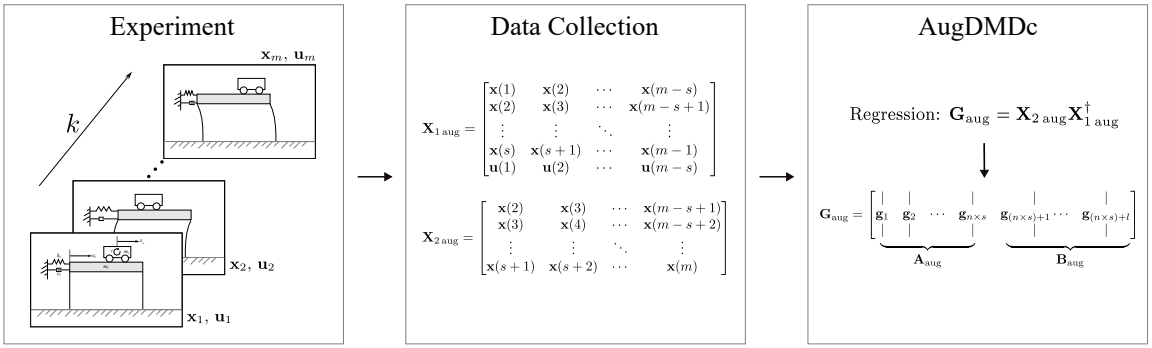

Figure 1: Schematic overview of the AugDMDc algorithm.

3 Structural dynamic example

This section presents the derivation of a toy example of a second-order state-space model of a structural dynamic system with an Active Mass Damper (AMD) on the last floor given in Fig. 2. We use this model to generate synthetic data to later test the capabilities and limitations of the DMD, DMDc, and DMDc with time-delay coordinates (AugDMDc) algorithms in a systematic and controlled manner. Several assumptions are considered for simplification. First, the input to the system will be a theoretical torque signal applied to the AMD to regulate its linear motion, as shown in Fig. 2. The linear motion of the AMD will generate oscillations in the structure similar to the ones present during earthquakes or in the presence of wind disturbances. This setting is slightly different from the actual conditions since, in the case of a real structure, we want to use the measured signal corresponding to the acceleration at the ground floor as input to our system. Second, for simplicity, assume access to the full state variables corresponding to position and velocity instead of the acceleration of the last floor are given. This simplification allows us to ignore the direct feedthrough from the torque input to the acceleration on the last floor. Nonetheless, for completeness, we present the derivation of the state space, including the output with direct feedthrough.

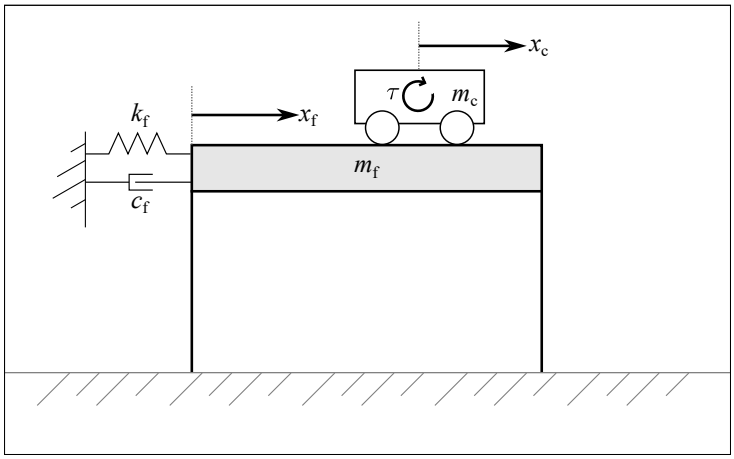

Figure 2: Simplified example of a structure with an AMD. The states of the system x_1 and x_2 correspond to the position x_f and velocity $\dot{x}_f$ of the building, respectively.

The structural dynamic system with an AMD showed in Fig. 2 can be described with the following equation as

$$-k_f x_f - c_f \dot{x}_f + m_c \ddot{x}_c = \ddot{x}_f m_f, \tag{22}$$

where $k_f = 500$ corresponds to the stiffness coefficient of the structure, $c_f = 3$ to the damping coefficient of the structure, $m_c = 0.39$ kg the mass of the AMD, and $m_f = 0.68$ kg to the mass of the last floor. The variables x_c and x_f correspond to the horizontal displacement of the AMD and the floor, respectively. Considering Eq. 22, and assuming as state vector $\mathbf{x}(t) = [\mathbf{x_1}(t)\ \mathbf{x_2}(t)]^T = [x_f\ \dot{x}_f]^T$ we derive a continuous-time state-space representation in the form of

$$\dot{\mathbf{x}}(t) = \mathbf{A}\mathbf{x}(t) + \mathbf{B}\mathbf{u}(t), \tag{23}$$

$$\mathbf{y}(t) = \mathbf{C}\mathbf{x}(t) + \mathbf{D}\mathbf{u}(t), \tag{24}$$

and with state matrices

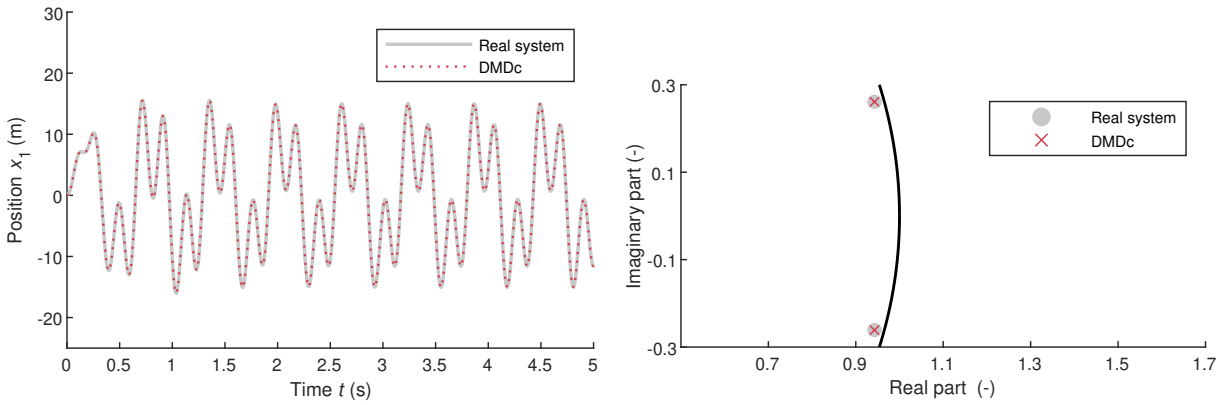

Figure 3: Left: Comparison of the measured and the DMDc simulated building position x_1. Right: Eigenvalues of the real system and the DMDc model.

$$\mathbf{A} = \begin{bmatrix} 0 & 1 \\ -k_\mathrm{f}/m_\mathrm{f} & -c_\mathrm{f}/m_\mathrm{f} \end{bmatrix}, \ \mathbf{B} = \begin{bmatrix} 0 \\ m_\mathrm{c}/m_\mathrm{f} \end{bmatrix}, \tag{25}$$

$$\mathbf{C} = \begin{bmatrix} -k_\mathrm{f}/m_\mathrm{f} & -c_\mathrm{f}/m_\mathrm{f} \end{bmatrix}, \text{ and } \mathbf{D} = \begin{bmatrix} 0 \\ \frac{1}{r m_\mathrm{c} m_\mathrm{f}} \end{bmatrix}, \tag{26}$$

where $\mathbf{u}(t)$ corresponds to the torque τ and $r = 6.3$ mm to the radius of the motor. Finally, we discretize the system in Eq. 23 using a zero-order holder to generate the synthetic data to deploy the DMD algorithms.

4 Results and Discussion

A key advantage of DMDc is its ability to separate a system's intrinsic dynamics from the influence of external inputs. When identifying system behavior from measurement data, it is often necessary to determine how the system evolves independently of external inputs. This distinction is particularly important in cases where actuation cannot be controlled or systematically varied, requiring analysis based solely on available data. Fig. 3 (left) demonstrates that DMDc achieves a high-accuracy reconstruction of the system, providing independent estimates of both the state-space matrix and the input matrix. The method effectively captures the system's natural behavior while accounting for external actuation, resulting in a nearly perfect reconstruction of the original signal. Moreover, the eigenvalues of the real system closely align with those of the DMDc model, as shown in Fig. 3 (right), confirming that the method accurately identifies the underlying system dynamics.

DMD struggles with noise, often failing to accurately identify system dynamics when measurement data are corrupted. The same limitation applies to DMDc, as it inherits this sensitivity to noise. Fig. 4 (left) illustrates the effect of noise on the DMDc reconstruction, showing that when noise is present, the reconstructed signal is significantly degraded. Examining the eigenvalues of the identified system in Fig. 4 (right) further highlights this issue. A clear mismatch is observed when comparing the eigenvalues of the DMDc-identified system to those of the original system. Specifically, the identified system exhibits much stronger damping than the true system, a common issue that arises in noisy conditions.

To mitigate the impact of noise, we introduce time-delay coordinates to the data and apply the AugDMDc algorithm as outlined in the previous section. The results, shown in Fig. 5, demonstrate that by incorporating 96 delay coordinates, we are able to effectively suppress the influ-

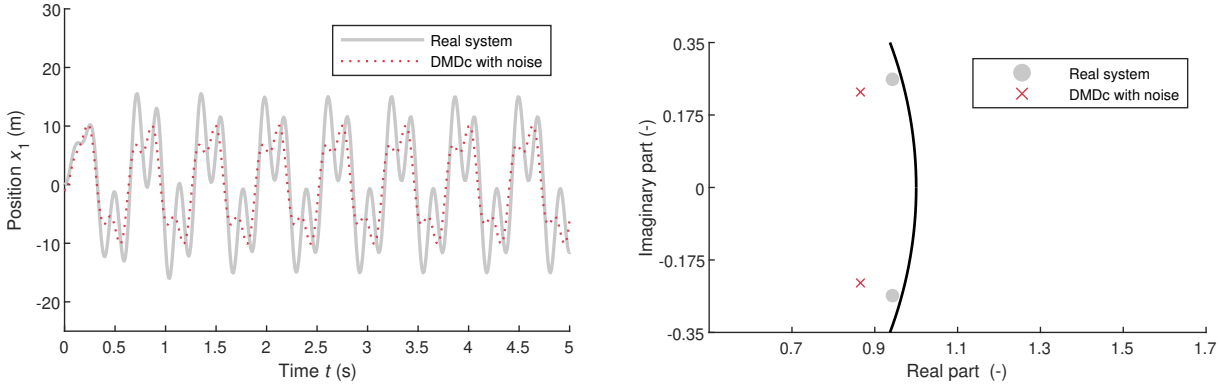

Figure 4: Left: The effect of noise on the DMDc reconstruction, showing significant degradation of the signal. Right: Eigenvalues of the DMDc-identified system compared to those of the original system.

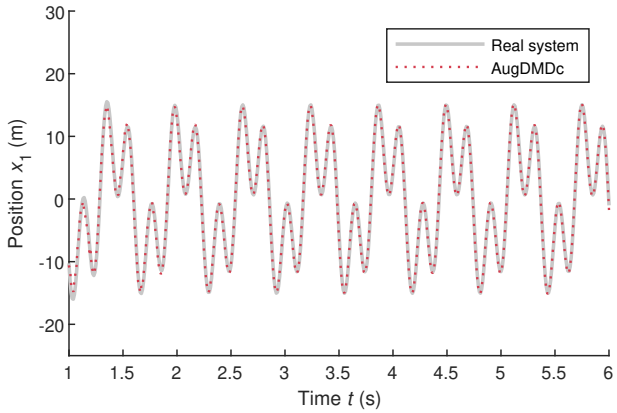

Figure 5: Comparison of the measurements and the AugDMDc reconstruction with 96 delay coordinates.

ence of noise and accurately reconstruct the original system dynamics. This highlights a key advantage of AugDMDc, as it addresses one of the primary limitations of classical DMDc—its sensitivity to noise. By leveraging time-delay coordinates, AugDMDc enhances the robustness of system identification, allowing for a more reliable identification of intrinsic dynamics even in the presence of significant measurement noise.

A fundamental objective of DMDc is to identify a system representation that decouples its intrinsic dynamics from the influence of external inputs. However, under certain conditions, this separation is not achieved. Instead, the algorithm may generate a system that attempts to reproduce the entire dataset as a whole, incorporating the external actuation as part of the identified system dynamics. When this occurs, the resulting input matrix is nearly zero, meaning that while the identified system can accurately replicate the observed data, it does not correctly capture how the system would respond to a different external input. The problem becomes particularly pronounced when an excessive number of delay coordinates is employed, arising in both noisy and non-noisy data. As demonstrated in Fig. 6 (left) (for noisy data) and Fig. 6 (right) (for non-noisy data), applying a large number of delay coordinates yields a free response that closely mirrors the provided dataset, implying that the system's behavior is insensitive to changes in external input. Rather than isolating the input effects, the algorithm effectively absorbs them into the system's dynamics. A possible way to mitigate this issue is to ensure that the excitation signal provided to the system is sufficiently rich, spanning a broad spectrum of amplitudes and frequencies. However, in many practical cases, control over the external input is limited or entirely unavailable. Therefore, it is crucial to verify whether the identified system

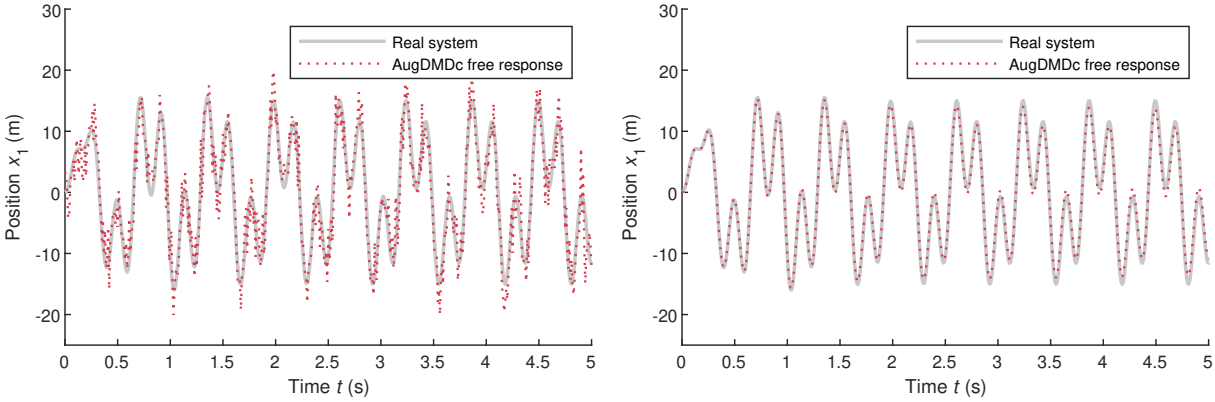

Figure 6: Comparison of measurements and free response. Left: AugDMDc with 500 delays (noisy data). Right: AugDmdc with 40 delays (non-noisy data).

is truly decoupled or if it has absorbed the input dynamics into its state evolution.

5 Conclusion

This study presents a data-driven strategy for vibration control in structures using DMDc and AugDMDc, addressing critical challenges in noise sensitivity and system identification. Key findings reveal that DMDc successfully isolates structural dynamics from external seismic inputs, enabling precise eigenvalue estimation. However, noise-corrupted data degrade DMDc's performance, leading to exaggerated damping ratios. AugDMDc resolves this by leveraging time-delay coordinates, improving noise robustness and accurately reconstructing system dynamics even with significant measurement noise.

Several open questions remain in the further development of these methods. One critical challenge is determining how the number of required delay coordinates relates to the level of noise in the data. Establishing a mathematical framework to determine the optimal amount of delay for accurate system identification is essential, as this would allow us to better understand how noise influences the delay requirements. Additionally, understanding the threshold beyond which too many delays result in external inputs being incorporated into the system's dynamics is necessary to ensure that the algorithm isolates the system's true behavior. Another major issue is the sensitivity of time-delay methods to sampling frequency. Because time-delay techniques rely on stacking delayed measurements, their effectiveness varies with the sampling frequency. The investigation into which frequencies are effective or fail will be continued in future research. Developing a method to identify the optimal sampling frequency is essential for ensuring the reliability of this approach across different experimental setups.

REFERENCES

[1] F. Casciati, J. Rodellar, and U. Yildirim. Active and semi-active control of structures – theory and applications: A review of recent advances. *Journal of Intelligent Material Systems and Structures*, 23(11):1181–1195, 2012.

[2] A. Di Matteo, C. Masnata, and A. Pirrotta. Hybrid passive control strategies for reducing the displacements at the base of seismic isolated structures. *Frontiers in Built Environment*, 5:1–13, 2019.

[3] F.Y. Cheng, H. Jiang, and K. Lou. *Smart Structures: Innovative Systems for Seismic Response Control*. CRC Press, 1st edition, 2008.

[4] S. Elias and V. Matsagar. Research developments in vibration control of structures using passive tuned mass dampers. *Annual Reviews in Control*, 44:129–156, 2017.

[5] T.T. Soong and G.F. Dargush. Passive energy dissipation systems in structural engineering. *Meccanica*, 34(1):65–66, 1999.

[6] M.J. Hudson and P. Reynolds. Implementation considerations for active vibration control in the design of floor structures. *Engineering Structures*, 44:334–358, 2012.

[7] M. Jafari and A. Alipour. Methodologies to mitigate wind-induced vibration of tall buildings: A state-of-the-art review. *Journal of Building Engineering*, 33:101582, 2021.

[8] S. Korkmaz. A review of active structural control: challenges for engineering informatics. *Computers Structures*, 89(23):2113–2132, 2011.

[9] B. Peeters and G. de Roeck. Reference-based stochastic subspace identification for output-only modal analysis. *Mechanical Systems and Signal Processing*, 13(6):855–878, 1999.

[10] R. Brincker, L. Zhang, and P. Andersen. Modal identification of output-only systems using frequency domain decomposition. *Smart Materials and Structures*, 10(3):441, 2001.

[11] G. Kerschen, K. Worden, A.F. Vakakis, and J. Golinval. Past, present and future of nonlinear system identification in structural dynamics. *Mechanical Systems and Signal Processing*, 20(3):505–592, 2006.

[12] P. J. Schmid. Dynamic mode decomposition of numerical and experimental data. *Journal of Fluid Mechanics*, 656:5–28, 2010.

[13] J.H. Tu, C.W. Rowley, D.M. Luchtenburg, S.L. Brunton, and J.N. Kutz. On dynamic mode decomposition: Theory and applications. *Journal of Computational Dynamics*, 1(2):391–421, 2014.

[14] J.L. Proctor, S.L. Brunton, and J.N. Kutz. Dynamic Mode Decomposition with Control. *SIAM Journal on Applied Dynamical Systems*, 15(1):142–161, 2016.

[15] S.L. Brunton, J.L. Proctor, and J.N. Kutz. Sparse identification of nonlinear dynamics with control (sindyc). *IFAC-PapersOnLine*, 49(18):710–715, 2016.

[16] A. Narasingam and J. S. Kwon. Development of local dynamic mode decomposition with control: Application to model predictive control of hydraulic fracturing. *Computers Chemical Engineering*, 106:501–511, 2017. ESCAPE-26.

[17] D. Duke, J. Soria, and D. Honnery. An error analysis of the dynamic mode decomposition. *Experiments in Fluids*, 52(2):529–542, 2012.

[18] Z. Wu, S. L. Brunton, and S. Revzen. Challenges in dynamic mode decomposition. *Journal of the Royal Society Interface*, 18(185):20210686, 2021.

[19] M.S. Hemati, C.W. Rowley, E.A. Deem, and L.N. Cattafesta. De-biasing the dynamic mode decomposition for applied koopman spectral analysis of noisy datasets. *Theoretical and Computational Fluid Dynamics*, 31(4):349–368, 2017.

[20] L. Lortie and J.R. Forbes. Asymptotically stable data-driven koopman operator approximation with inputs using total extended dmd. *Machine Learning: Science and Technology*, 6(1), 2025.

[21] J.N. Kutz, S.L. Brunton, B.W. Brunton, and J.L. Proctor. *Dynamic Mode Decomposition: Data-Driven Modeling of Complex Systems*. Society of Industrial and Applied Mathematics, Philadelphia, 2016.

[22] S. Brunton and J. Kutz. *Data-driven science and engineering: machine learning, dynamical systems, and control*. Cambridge University Press, Cambridge, 2022.

[23] F. Takens. Detecting strange attractors in turbulence. In *Dynamical Systems and Turbulence, Warwick 1980*, pages 366–381, Berlin, Heidelberg, 1981. Springer Berlin Heidelberg.